Structural Engineering and Mechanics, *Vol. 66, No. 1 (2018) 85-96*
DOI: https://doi.org/10.12989/sem.2018.66.1.085

Nonlinear transient analysis of FG pipe subjected to internal pressure and unsteady temperature in a natural gas facility

Ahmed E. Soliman[2], Mohamed A. Eltaher[*1,2], Mohamed A. Attia[2,3] and Amal E. Alshorbagy[2]

[1]*Department of Mechanical Engineering, Faculty of Engineering, King Abdulaziz University, P.O. Box 80204, Jeddah 21589, Saudi Arabia*
[2]*Department of Mechanical Design and Production, Faculty of Engineering, Zagazig University, Egypt*
[3]*Department of Mechanical Engineering, College of Engineering, Shaqra University, Dawadmi, Saudi Arabia*

(Received August 19, 2017, Revised January 28, 2018, Accepted January 29, 2018)

Abstract. This study investigates the response of functionally graded (FG) gas pipe under unsteady internal pressure and temperature. The pipe is proposed to be manufactured from FGMs rather than custom carbon steel, to reduce the erosion, corrosion, pressure surge and temperature variation effects caused by conveying of gases. The distribution of material graduations are obeying power and sigmoidal functions varying with the pipe thickness. The sigmoidal distribution is proposed for the 1st time in analysis of FG pipe structure. A Two-dimensional (2D) plane strain problem is proposed to model the pipe cross-section. The Fourier law is applied to describe the heat flux and temperature variation through the pipe thickness. The time variation of internal pressure is described by using exponential-harmonic function. The proposed problem is solved numerically by a two-dimensional (2D) plane strain finite element ABAQUS software. Nine-node isoparametric element is selected. The proposed model is verified with published results. The effects of material graduation, material function, temperature and internal pressures on the response of FG gas pipe are investigated. The coupled temperature and displacement FEM solution is used to find a solution for the stress displacement and temperature fields simultaneously because the thermal and mechanical solutions affected greatly by each other. The obtained results present the applicability of alternative FGM materials rather than classical A106Gr.B steel. According to proposed model and numerical results, the FGM pipe is more effective in natural gas application, especially in eliminating the corrosion, erosion and reduction of stresses.

Keywords: finite element method; FG Pipe; natural gas industry; nonlinear transient analysis; unsteady pressure and temperature

1. Introduction

In exploration and conveyance of natural gas industry, high speed of soft sand particles, salts and sulfur cause failure of inner surface of pipes by corrosion and erosion. In normal (start-up, shutdown) and unexpected operation conditions, created wave shocks will cause high variations and fluctuations in both temperature and pressure inside the pipe. Highly change in both temperature and pressure may cause failure of traditional carbon steel A106Gr.B pipe. So that, new generations of material such as a graded material should replace the traditional carbon steel pipe. Functionally graded materials (FGMs) are considered a special class of composite materials characterized by smooth and continuous distribution of material properties. They have comparatively smaller residual stresses, lower stress concentrations, and higher bonding strength than conventional composite laminates, Aldousari (2017). The FGM concept originated in Japan in 1984 during the space-plane project, in the form of a proposed thermal barrier material capable of withstanding a surface temperature of 2000 K, (Alshorbagy *et al.* 2011). FGM is proposed to overcome the erosion, corrosion and temperature variation because it is formed from metallic and ceramic materials. In the petroleum industry, shell is the most important structure, which is used in different applications such as pipelines, piping, storage tanks, and pressure vessels. Transient analysis is important in designing of structures that work under thermomechanical load time dependent and pressure fluctuations.

Within the framework of the functional graded shell structures modeling, Aboudi *et al*. (1999) presented full generalization of higher-order theory of functionally graded materials by explicitly coupling the local (microstructural) and global (macrostructural) responses. Chareonsuk and Vessakosol (2011) proposed a high-order control volume finite element method to explore thermal stress analysis for functionally graded materials (FGMs) at steady state. The heat conduction was considered for thermal analysis whereas the plane elasticity was considered for stress analysis. Liew *et al.* (2011) presented a review of element meshless methods for laminated and functionally graded plates and shells. Fu *et al.* (2014) investigated transient deformation of FG shallow spherical shells subjected to time-dependent thermomechanical load and based on Timoshenko Mindlin hypothesis and von Karman nonlinear theory. Liang *et al.* (2015) investigated the elastic dynamic responses of FG plates to underwater shock by fluid solid interaction model and solved problem analytically by using

*Corresponding author, Associate Professor
E-mail: mohaeltaher@gmail.com or meltaher@kau.edu.sa or mmeltaher@zu.edu.eg

ISSN: 1225-4568 (Print), 1598-6217 (Online)

Laplace transform and state space methods. Kar and Panda (2015) investigated free vibration of shear deformable FG single/doubly curved panels under uniform, linear and nonlinear temperature fields. The micromechanical material modeled by Voigt theory in conjunction with the power-law distribution to achieve the continuous gradation. Thai and Kim (2015) provided a review for the existing theories of functionally graded plates and shells to predict the global responses under mechanical and thermal loadings.

Abdelhak *et al.* (2016) studied thermal buckling behavior of functionally graded (FG) sandwich plates using higher shear deformation theory. Material characteristics and thermal expansion coefficient of the sandwich plate faces are considered to be graded in the thickness direction according to a simple power-law distribution in terms of the volume fractions of the constituents. Fazzolari (2016) proposed a mixed displacements-transverse stresses approach for the free vibration analysis of FGM doubly-curved shells. Chikh *et al.* (2016) studied thermo-mechanical postbuckling of symmetric functionally graded plates resting on Pasternak elastic foundations using hyperbolic shear deformation theory. Jafari Fesharaki *et al.* (2016) developed thermo-elastic analysis of FG cylinder under thermomechanical loadings. Thermal conductivity was assumed to be graded along the radial direction and heat conduction equation was solved in cylindrical coordinate system. Viola *et al.* (2016) presented static behavior of functionally graded spherical shells and panels subjected to uniform loadings at the extreme surfaces by means of the unconstrained 3rd order shear deformation theory and the posteriori stress and strain recovery procedure. Wu and Lim (2016) investigated electro-mechanical coupling effects and dynamic responses of FG piezoelectric film-substrate circular hollow cylinders. Functionally graded piezoelectric material layer was assumed to obey an exponent-law exponentially varying with the thickness coordinate. Ranjbar and Alibeigloo (2016) presented an analytical solution to analysis dynamic behavior of FG thick hollow sphere subjected to thermo-mechanical timed dependent load. Moosaie (2016) performed an uncoupled nonlinear thermo-elastic analysis of a thick-walled FG cylinder with temperature dependent material properties. The heat conduction equation was solved analytically by the perturbation method. Khazaeinejad and Usmani (2016) formulated theoretically the temperature dependent nonlinear response of shallow shells with single and double curvatures subjected to transverse mechanical loads while being exposed to through-depth non-uniform fire heating regimes. Tounsi *et al.* (2016) presented a new 3-unknown non-polynomial shear deformation theory for the buckling and vibration analyses of functionally graded material (FGM) sandwich plates. Hamed *et al.* (2016) investigation of vibration characteristics of both nonlinear symmetric power and sigmoid functionally graded nonlocal nanobeams.

Sator *et al.* (2017) studied coupling effects of multi-gradation material coefficients in FGM plates. (She *et al.* 2017) predicted the nonlinear bending behaviors of FGM infinite shallow shells rested on two-parameter elastic foundations and subjected to uniform temperature rise. Sheng and Wang (2017) studied nonlinear dynamic

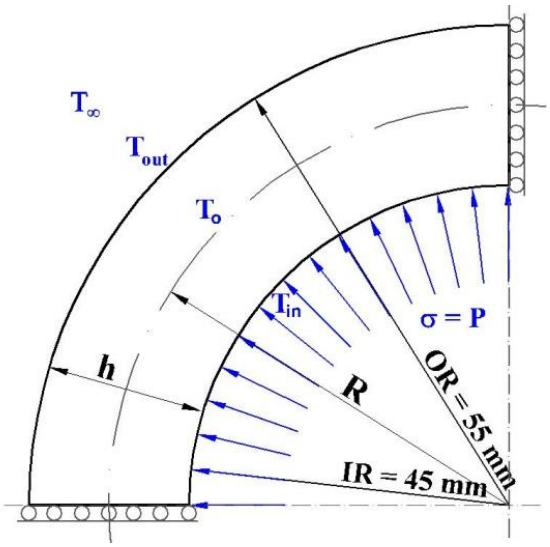

Fig. 1 Geometry of pipe cross section

behavior of the fluid-conveying power functional graded cylindrical shell included the thermal effects and assumed material properties to be temperature-dependent. Wu and Liu (2017) presented comprehend review of semi-analytical numerical methods for quasi-three-dimensional (3D) analyses of laminated composite and multilayered functionally graded materials plates and shells with different boundary conditions. Ghannad and Yaghoobi (2017) studied a steady state thermo-elastic response of axisymmetric FG cylinder subjected to pressure and external heat flux in inner surface displacement field. Najibi and Talebitooti (2017) investigated transient thermo-elastic response of a thick hollow two dimensional functionally graded cylinder by utilizing finite element method. Daneshjou *et al.* (2017) studied wave propagation and transient response of a fluid-filled FGM varying smoothly and continuously across the thickness of rigid core cylinder using the Laplace transform. Akbarov *et al.* (2017) investigated natural vibration of the three-layered hollow sphere with middle layer made of FGM by using Three-dimensional exact field equations of elastodynamics.

From the literature review and to the best of the authors' knowledge, it is a first attempt to consider nonlinear transient response of sigmoidal function graded shell structure under unsteady pressure and transient temperature. This paper is organized as follows: Section 2 describes material graduation functions, 2D plane strain constitutive equation, pressure function, temperature distribution and heat equations. Section 3 summarizes the governing equilibrium equations and finite element scheme. Numerical results and concluding remarks are presented in Sections 4 and 5, respectively.

2. The Mathematical model formulation

2.1 Geometry description

Fig. 1 shows the cross section of a pipe with 110 mm outer diameter similar to that is used in a natural gas facility. The mean radius is R=50 mm, and pipe thickness is

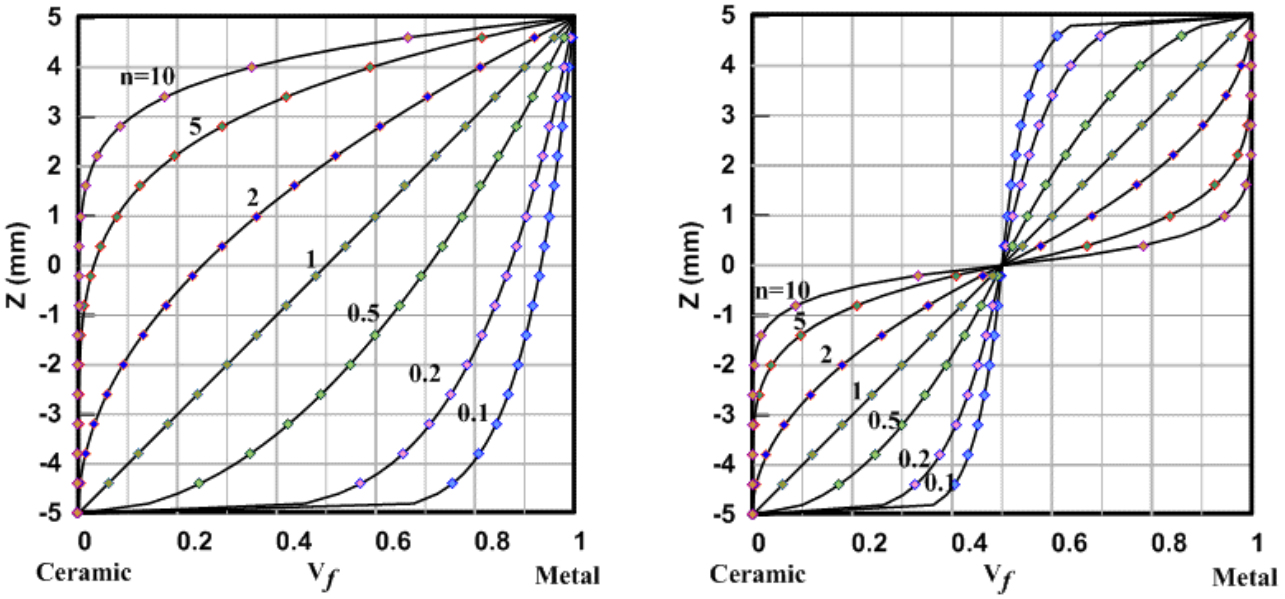

(a) Power-FGM (b) Sigmoid-FGM

Fig. 2 The variation of the volume fraction through thickness at different exponent values

Table 1 Materials properties of the metal (Carbon steel A106Gr.B) and the ceramic (alumina, Al_2O_3)

Properties	Ultimate tensile strength (GPa)	Yield strength (GPa)	Mass density (kg/m^3)	Young's modulus (GPa)	Poisson's ratio	Specific heat (J/kgK)	Thermal Conductivity (W/m.K)	Thermal expansion Coefficient, (/K)
A106Gr.B	0.415	0.24	7850	240	0.3	461	51	1.25E-05
Alumina	0.665	0.665	3800	380	0.3	880	10.4	7.40E-06

h=10 mm, $-\frac{h}{2} \le z \le \frac{h}{2}$, (i.e., $-5 \le z \le 5$). Due to symmetry conditions, only one-quarter of the cross-section profile is used in the FE model of the problem.

2.2 Material characteristics

The most popular graduation assumed in FGMs is the power law distribution, so it is proposed in the current analysis. Also, to reduce the stress intensity factors combination of two types of power functions which is known as sigmoidal function is assumed, Chi and Chung (2002). The material properties such as, density (ρ), modulus of elasticity (E), Poisson ratio (ν), thermal conductivity (k), specific heat (c) and thermal expansion coefficient (α) can be described as a power function as following

$$P(z) = P_c + (P_m - P_c)V_f \qquad V_f = \left(\frac{z}{h} + \frac{1}{2}\right)^n \tag{1}$$

In which P is the material property, the exponent n is the parameter of material distribution, V_f is the volume fraction of metal and it is inversely proportional to n. P_m and P_c are the metal and ceramic properties, respectively. In case of sigmoidal function distribution, the material properties can be depicted by the following two power functions

$$P(z) = G_1(z)P_1 + [1 - G_1(z)]P_2$$

$$G_2(z) = \frac{1}{2}\left(\frac{\frac{h}{2} + z}{\frac{h}{2}}\right)^n \qquad for\ 0 \le z \le \frac{h}{2} \tag{2a}$$

$$P(z) = G_2(z)P_1 + [1 - G_2(z)]P_2$$

$$G_2(z) = \frac{1}{2}\left(\frac{\frac{h}{2} + z}{\frac{h}{2}}\right)^n \qquad for -\frac{h}{2} \le z \le 0 \tag{2b}$$

The variation of the volume fraction through the thickness at different n values in case of power and sigmoidal functions are shown in Fig. 2.

Therefore, a sigmoid FGM, which is composed of two power law, functions to define a new volume fraction is used and Chi and Chung (2002) indicated that the use of a sigmoid FGM can significantly reduce the stress intensity factors of a cracked body. The proposed materials are Carbon steel (A106Gr.B) as a metal which has more ductility, better thermal conductivity, lower specific heat and lower stiffness; and alumina (Al_2O_3) as ceramics which has corrosion resistance, better toughness, lower expansion coefficient and lower density. The material properties of these materials are presented in Table 1.

2.3 Governing equation

To analyze the thermoelastic behaviour of a pipe, plane strain problem can be assumed to describe the constitutive behaviour in cylindrical coordinate as,

(3a)

$$\sigma_z = \frac{\nu E}{(1+\nu)(1-2\nu)}(\varepsilon_r+\varepsilon_\theta) \quad (3b)$$

where σ_r, σ_θ and $\sigma_{r\theta}$ are, respectively, the component of the radial stress, hoop stress and shear stress, ε_r and ε_θ are the normal strain components at the radial and hoop directions, respectively, and $\varepsilon_{r\theta}$ is the shear strain component.

The geometrical fit conditions can be defined as

$$\varepsilon_r = \frac{\partial u_r}{\partial r},\ \varepsilon_\theta = \frac{u_r}{r} + \frac{1}{r}\frac{\partial u_\theta}{\partial \theta}\ ,\ 2\varepsilon_{r\theta} = \frac{1}{r}\frac{\partial u_r}{\partial \theta} + \frac{\partial u_\theta}{\partial r} - \frac{u_\theta}{r} \quad (4)$$

where u_r is the component of displacement at the radial direction, u_θ is the component of displacement at the hoop direction, θ is the angle, and r is the radius.

2.4 The governing equations

The dynamic equilibrium equation of a hollow cylinder, disregarding the body forces, is

$$\frac{\partial \sigma_r}{\partial r} + \frac{\sigma_r - \sigma_\theta}{r} = \rho(r)\frac{\partial^2 u}{\partial t^2} \quad (5)$$

and transient heat conduction can be determined by

$$\frac{1}{r}\frac{\partial}{\partial r}\left(rk(r)\frac{\partial T(r,t)}{\partial r}\right) + \frac{1}{r^2}\frac{\partial}{\partial \theta}\left(k(r)\frac{\partial T(r,t)}{\partial \theta}\right) = \rho(r)C(r)\frac{\partial T(r,t)}{\partial t} \quad (6)$$

in which k, ρ, C are the thermal conductivity, mass density and heat capacity respectively.

2.5 Dynamic pressure load and temperature variation

Due to irregular behaviour of dynamic pressure load of the natural gas in piping, the pressure load function is assumed to follow

$$P = P_o \times \left(1 + \frac{sin(2\times t)}{e^{\left(\frac{t}{10}\right)}}\right) \quad N/m^2 \quad (7)$$

where, P is the gas pressure inside the pipe and P_o is the steady state pressure, P_o= 125 x10^5 Pa. The variation of the pressure with time is presented in Fig. 3. The time variation of the inner surface temperature is assumed according to the exponential equation as

$$T_s = T_n - (T_n - T_o).e^{-\gamma t} \quad (8)$$

where T_s is the inner surface temperature, T_o and T_n are the inner surface initial and eventual temperatures, respectively and γ is a coefficient describing the rate of temperature change. In the current analysis, it is assumed that T_o = 27°C, T_n = 75°C and γ = 0.1.

2.6 Boundary conditions

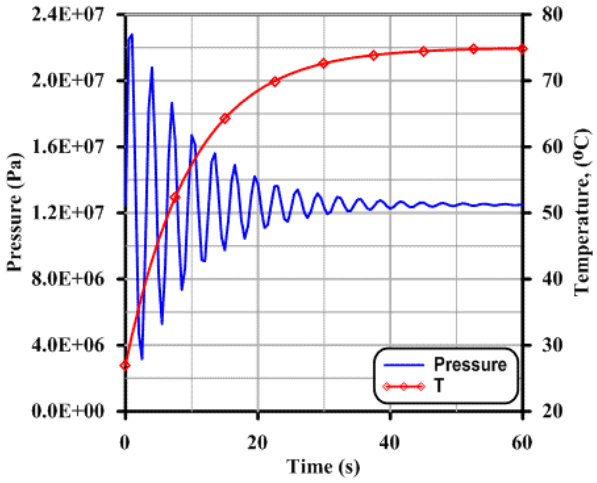

Fig. 3 The variation of dynamic pressure and unsteady temperature with time

The geometrical boundary conditions of a hollow cylinder can be described by

$$u_\theta(r,0) = u_\theta\left(r,\frac{\pi}{2}\right) = 0 \quad (9)$$

and the thermal boundary conditions can be represented by

$$k\frac{\partial T(r_o)}{\partial r} + h_o(T - T_\infty) = 0 \quad (10a)$$

$$T(r,\theta,0) = T_o \quad (10b)$$

Assuming that the initial temperature of pipe is T_o = 27°C and the atmospheric temperature is T_∞= 27°C and the convection coefficient is h_o = 50 W/m.K.

3. Numerical formulation

Through this analysis the nonlinear model of a sigmoidal function graded pipe is solved by using finite element software of ABAQUS, which has a higher accuracy in analysis of solid structure. The nine node isoparametric quadrilateral finite element is selected from ABAQUS library. The stresses in the quadrilateral element are not constant within the element; the stresses are evaluated at the Gaussian integration points of the element. Quadrilateral shape has a better convergence rate and less effect by mesh orientation than triangles.

3.1 The coupled thermo-elastic analysis

Coupled thermo-elasticity equations are used to find a solution for the stress-displacement and temperature fields simultaneously when the thermal and mechanical solutions are affected greatly by each other. It is mainly valid for small temperature changes, but it has been used for relatively high temperature changes as well. Backward-difference method is used to integrate the temperatures heat transfer equations, and Newton's method is used in solving the nonlinear coupled system. Coupled equations non-symmetric Jacobian matrix is

$$\begin{bmatrix} K_{uu} & K_{u\theta} \\ K_{\theta u} & K_{\theta\theta} \end{bmatrix} \begin{Bmatrix} \Delta u \\ \Delta\theta \end{Bmatrix} = \begin{Bmatrix} R_u \\ R_\theta \end{Bmatrix} \quad (11)$$

Where Δu and $\Delta\theta$ are particular corrections of the incremental displacement and temperature, K_{ij} is a sub-matrices of the fully coupled Jacobian matrix and R_u , R_θ are the mechanical and thermal residual vectors. When the coupling between the two solutions is weak the off-diagonal sub-matrices are neglected.

$$\begin{bmatrix} K_{uu} & 0 \\ 0 & K_{\theta\theta} \end{bmatrix} \begin{Bmatrix} \Delta u \\ \Delta\theta \end{Bmatrix} = \begin{Bmatrix} R_u \\ R_\theta \end{Bmatrix} \quad (12)$$

The minimum usable time increment and the element size in transient analysis with second-order elements is $\Delta t > \frac{\rho c}{6k} \Delta l^2$, where Δt is time increment, ρ is mass density, c is specific heat, k is thermal conductivity and Δl is element dimension (length of its side).

3.2 Numerical integration method

For dynamic Analysis, the load vector has the form

$$F^N = -M^{NM}\ddot{u}^M_{t+\Delta t} + (1+\alpha)G^N_{t+\Delta t} - \alpha G^N_t \quad (13)$$

where M^{NM} is the element mass matrix, G^N is the static load vector and α is the Hughes-Hilbert-Taylor (HHT) integration operator.

$$M^{NM}\left(\frac{d\ddot{u}}{du}\right) + (1+\alpha)C^{NM}\left(\frac{d\dot{u}}{du}\right) + (1+\alpha)K^{NM} \quad (14)$$

where $\frac{d\ddot{u}}{du} = \frac{1}{\beta\Delta t^2}$ and $\frac{d\dot{u}}{du} = \frac{\gamma}{\beta\Delta t}$

The implicit numerical Newmark-β method is proposed through analysis where $\beta = \frac{(1-\alpha)^2}{4}$ and $\gamma = \frac{1}{2} - \alpha$ are Newmark-β coefficients.

FGM characteristics, dynamic fluctuation loads and unsteady temperature are formed by adopted FORTRAN program that is embedded in ABAQUS software through the user-defined subroutines UMAT, UMATH, UAMP and USDFLD. The user-defined subroutines UMAT and UMATH have been used to implement gradients of the mechanical properties such as the Young's modulus, Poisson's ratio and the coefficient of thermal expansion, and the graded thermal properties like conductivity and specific heat, respectively. While the user subroutine USDFLD defines the spatial variation of the mass density. The user subroutine UAMP defines the dynamic fluctuation pressure and unsteady temperature, Simulia (2012).

4. Numerical results

4.1 The validation of the method

For validation of the current model is compared with the results obtained by Chareonsuk and Vessakosol (2011) for a pressurized hollow FG cylinder as shown in Fig. 4(a) and the results obtained by Fu *et al.* (2014) for the transient response of a 2D FG thin shell under increasing temperature $T_t = T_0(1 - e^{-\gamma t})$ as shown in Fig. 4(b). Material

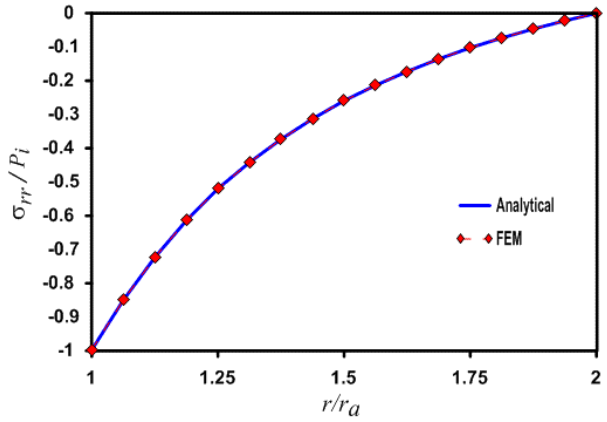

Fig. 4(a) Radial Stress in a pressurized hollow FG cylinder

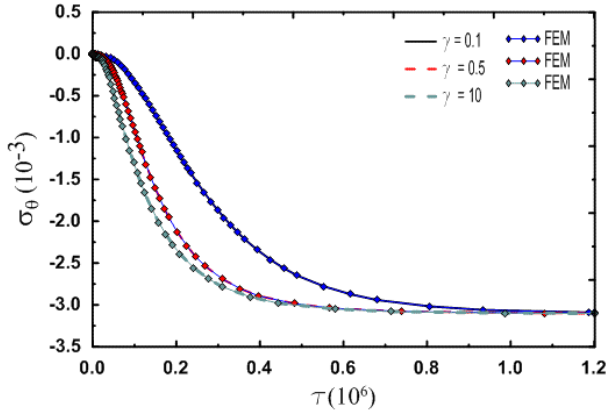

Fig. 4(b) Circumferential stress of a thin FG shell subjected to increased temperature

composition, geometry and boundary conditions are taken into consideration.

To study the stress features according to material composition variation under different loads, the response is obtained under the unsteady pressure load, thermal load and their simultaneous effect. The effective stress has been evaluated from the principal stresses using the von Mises-Hencky theory. Assuming that the initial temperature of pipe is T_o = 27°C and the atmospheric temperature is T_∞= 27°C and the convection coefficient is h_o = 50 W/m.K.

$$\sigma_e = \sqrt{\frac{1}{2}((\sigma_1 - \sigma_2)^2 + (\sigma_2 - \sigma_3)^{2+}(\sigma_3 - \sigma_1)^2)} \quad (15)$$

where σ_1, σ_2, σ_3 are the principal stresses.

A nonlinear transient fluctuating pressure has been applied to a FGM pipe subjected to unsteady change in the internal surface temperature and hence a change in the heat flux transfers through the pipe wall. In order to apply a transient fluctuation pressure through the pipe a transient pressure formulation is proposed. Elastic and thermo-elastic behavior has been studied by means of a FE analysis. Power function and sigmoidal function are studied to determine the FGM best configuration. The stresses at different time frames are investigated, in addition to the effect of FGM distribution and change in pressure and temperature magnitudes. Mechanical and thermal behavior of homogeneous pipes is included to illustrate the extent of

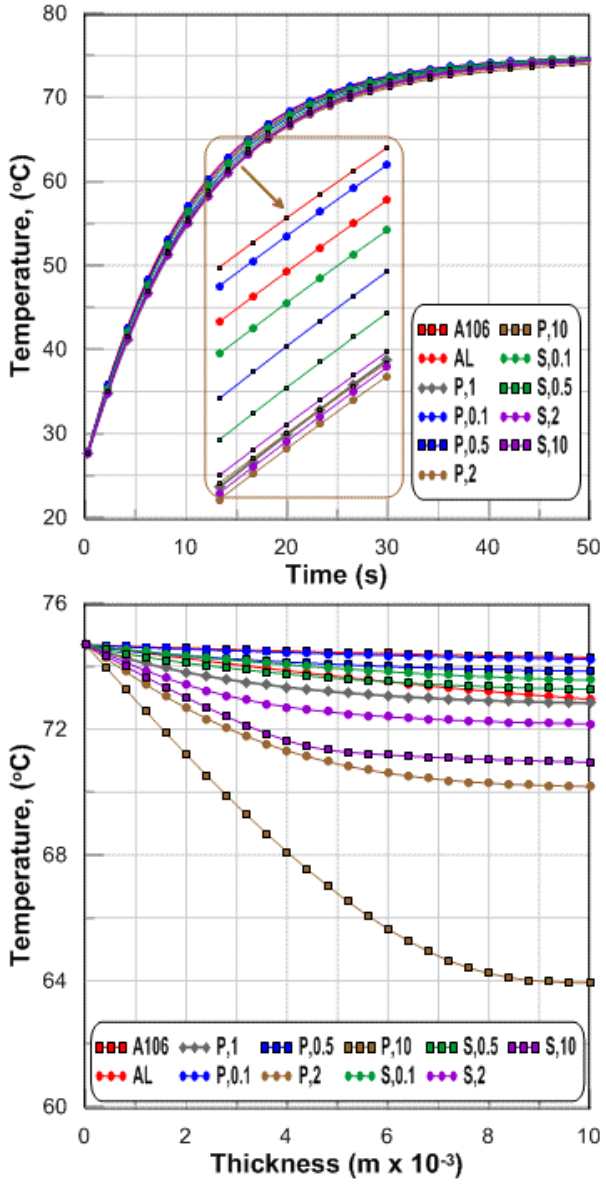

Fig. 7 Temperature graduation according to the material composition under thermal load

variation in the response gained by applying FGM. The outer surface of pipe has full thermal interaction with surroundings and the material composition changes gradually in the radial direction, so the temperature changes in the radial direction and it is equal at each layer in the circumferential direction. Stresses changes in the radial direction and are equal at each layer in the circumferential direction because of equal distribution of loads at each time frame as well as the material composition is changed only in the radial direction. Results obtained hereinafter are consistent with these features and emphasizes the applicability of FGM and the advantages of each distribution in the reduction of the equivalent stress and stress components. At pipeline design the failure happened at hoop direction comes from the pressure load and failure happened at axial direction come from thermal load expansion, so FGM response to these loads at axial and hoop direction are presented and discussed. In the following

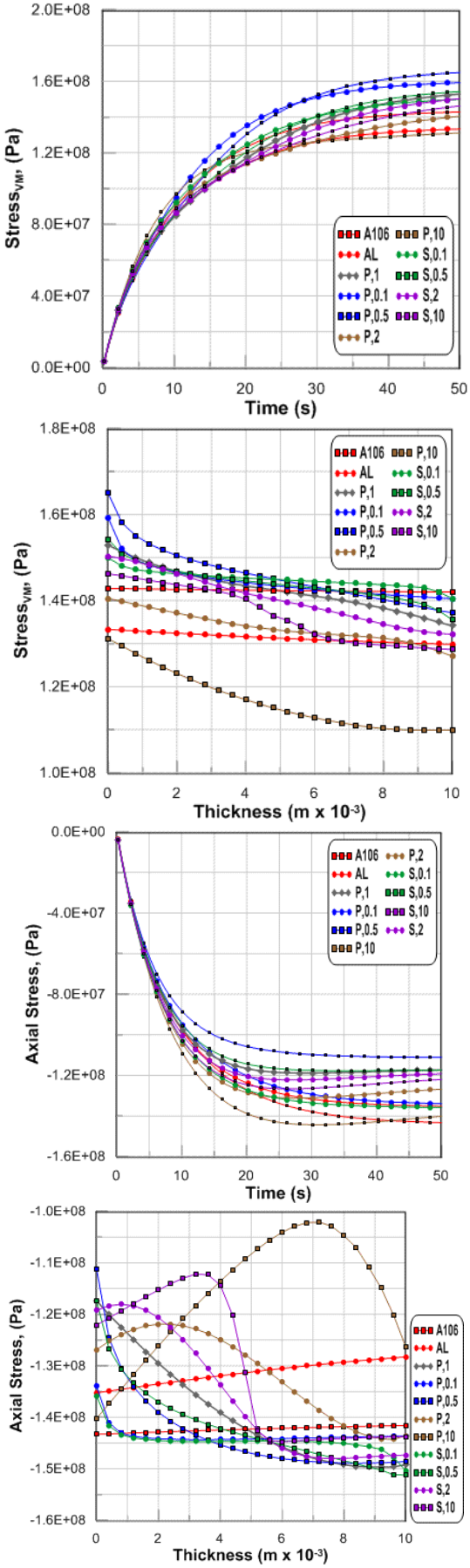

Fig. 8 Thermal stresses graduation according to the material composition

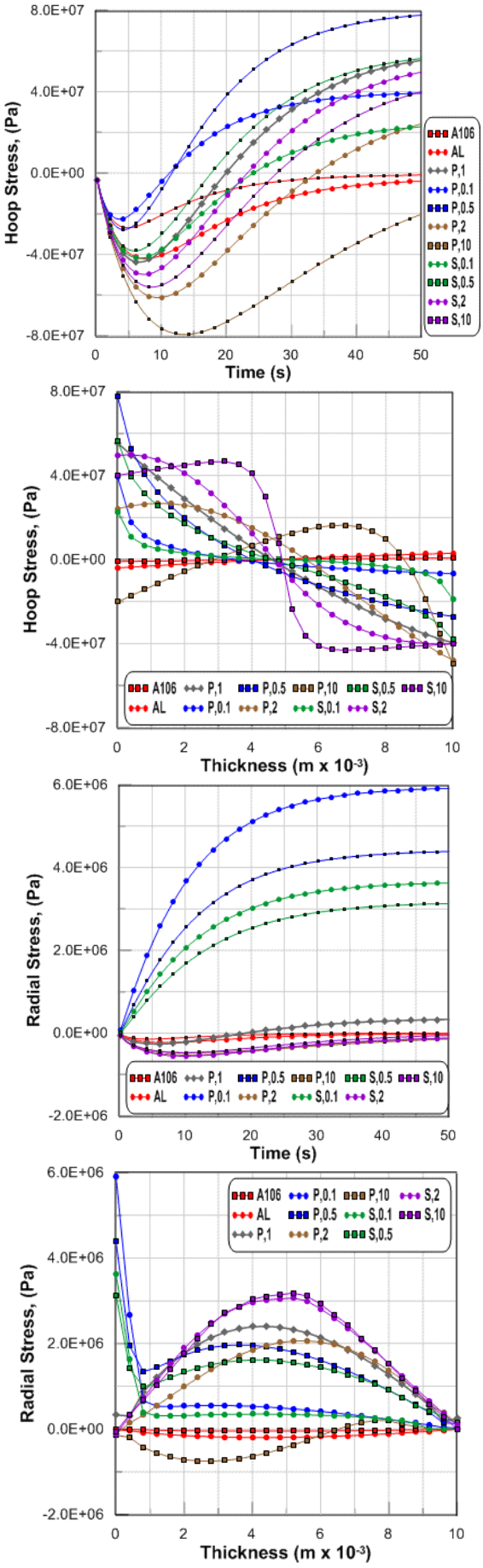

Fig. 8 Continued

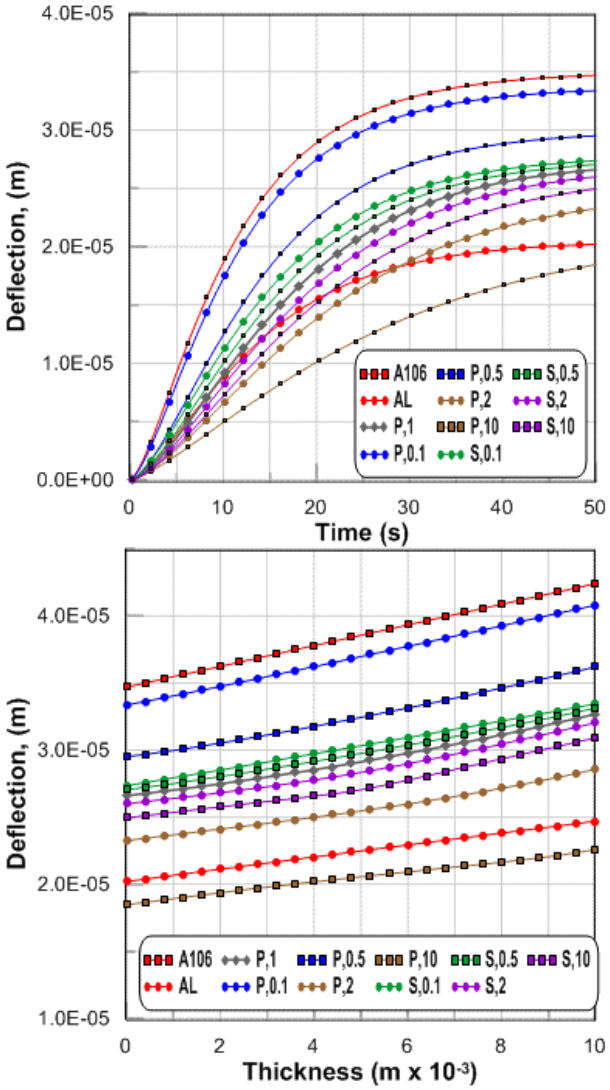

Fig. 9 Thermal deflection according to the material composition

figures A106 is the Carbon steel, Al is the alumina and P and S denotes the PFGM and SFGM respectively and is followed by the index value.

4.2 Effect of thermal load

Applying of the different FGM distributions leads to the illustrated graduation of temperature variation through the pipe wall at Fig. 7 Increasing power index attracts the material characteristics at the inner part towards the ceramic and at the outer part towards the metal, so the most temperature variation comes from PFGM, n=10. It is evident from these figures that both maximum values of distributions of the displacements and temperature are strongly affected by volume fractions indices

Analysis of stresses is shown in Fig. 8 at the radial, hoop and axial direction emphasis that when the power index is lower than one the stresses are increased specially for PFGM and SFGM is better. Contrary to that when the power index is more than one, the PFGM is the better and its stresses are lower. Thermal stresses effectively acts in

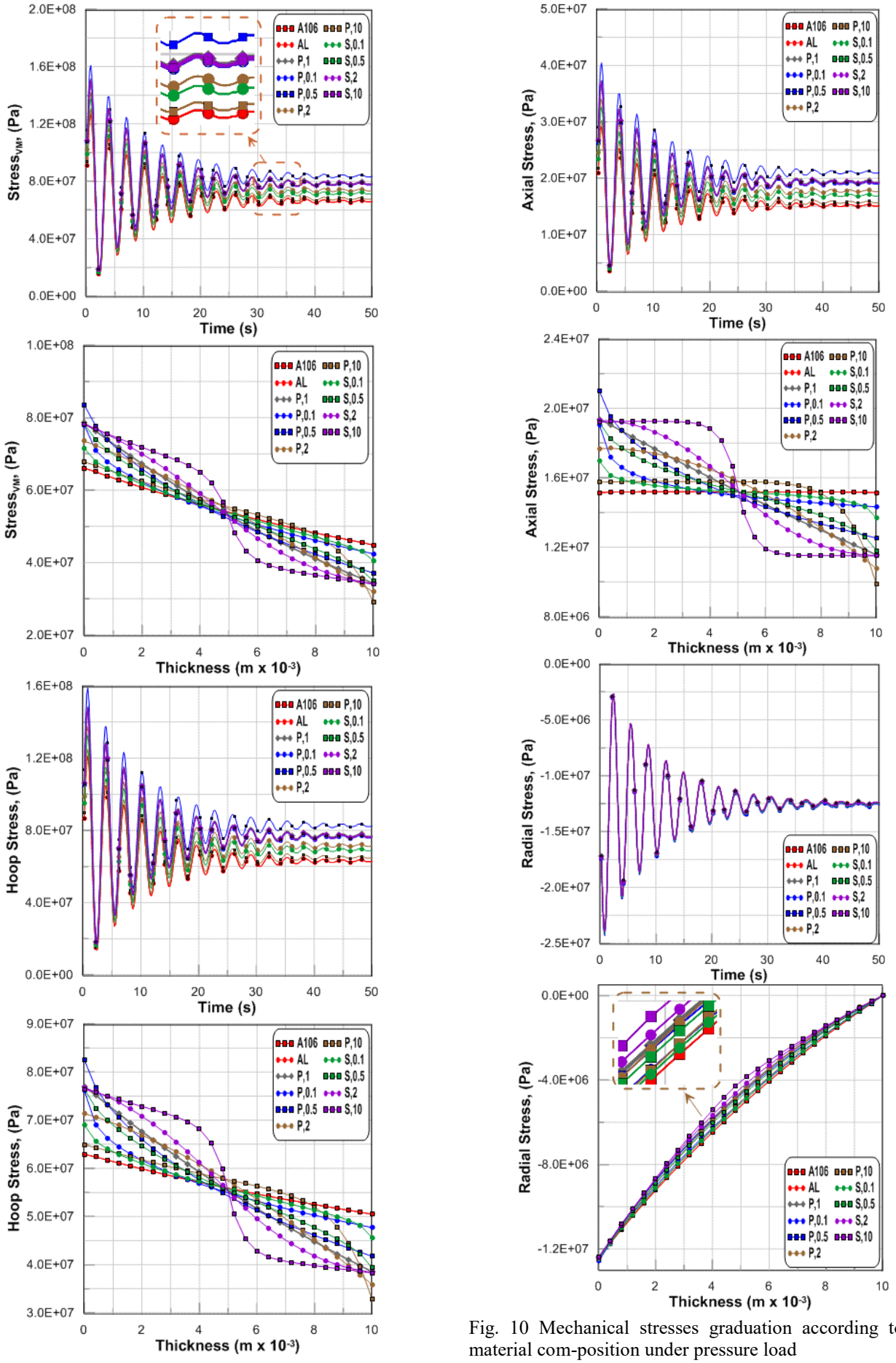

Fig. 10 Mechanical stresses graduation according to the material com-position under pressure load

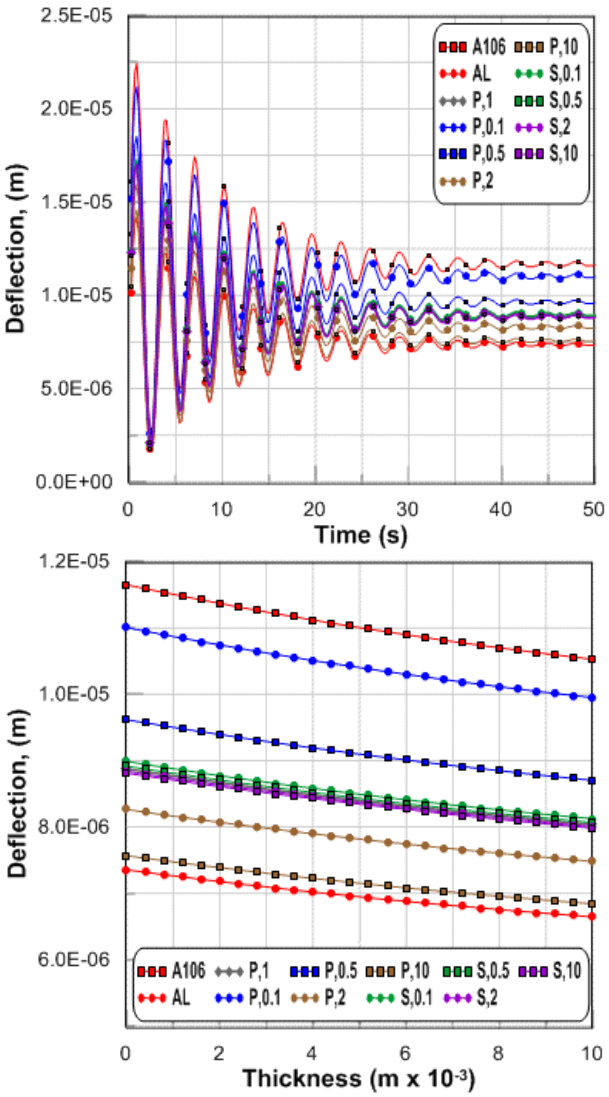

Fig. 11 Mechanical deflections according to the material composition under pressure load

the axial direction and its lower values are in the radial direction. PFGM, n=10 reduces the Von-Mises stresses to reach about 85% of the others through thickness. Carbon steel has the most deflection, whereas PFGM, n=10 has the most stiffness. The deflection of each material configuration is shown in Fig. 9.

4.3 Effect of pressure

Unlike the thermal stresses, the mechanical stresses are more effective in the hoop direction. The lowest stresses occurred at the homogeneous materials. However, PFGM, n=10 stress value is close to them as shown in Fig. 10. The hoop stress resulting from pressure load decreases continuously through the pipe wall from inside to outside and its reduction rate is related to the material configuration as it mainly depends on the modulus of elasticity; however, the hoop stress resulting from thermal load behaves in the same manner except at distribution begins with very rich ceramic as at PFGM with n=10 and SFGM with n=10, it increases first then reduces. This behavior is due to the

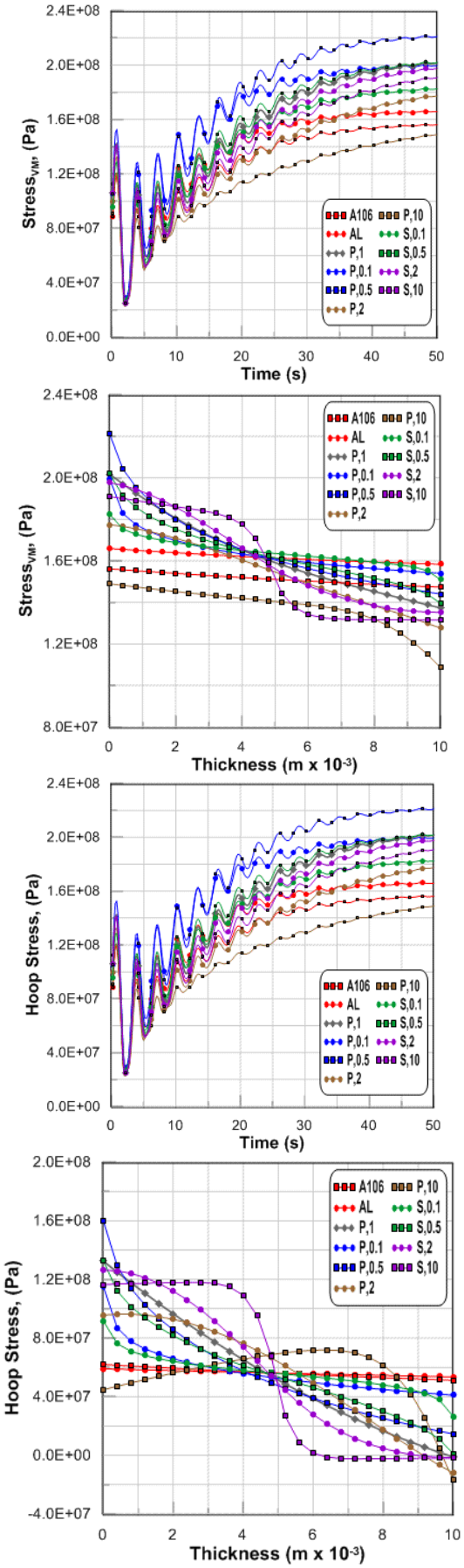

Fig. 12 Stresses graduation according to the material composition under combined load

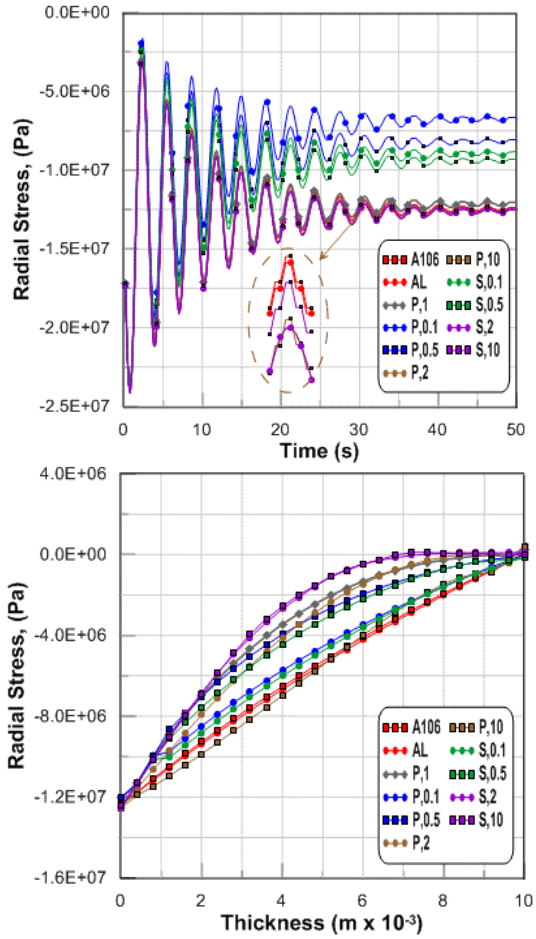

Fig. 12 Continued

thermal stress dependence on the expansion coefficient of material and the temperature which depends on the conductivity of material. Ceramic constituent has lower conductivity, lower expansion coefficient and higher specific heat than metal constituent. The lower the stress at the internal surface the greater at the outer surface in the same pipe, so FGM allows to redistribute the stresses in the pipe. A106Gr.B and Alumina have the same stresses resulted by internal pressure because the difference in their properties make the deflection at the carbon steel pipe 1.57 that at the alumina pipe whereas the deflection of FGM existed gradually between them according to the function and power index.

Fig. 11 illustrates that A106Gr.B has the most deflection, whereas Alumina has the lower deflection. The power index effects the deflection greatly and PFGM with n=10 deflection is greater than the alumina deflection.

4.4 Combined effect of thermal and pressure

In order to get a better view about the FGM characteristics, the thermal and pressure loads are combined and the stresses are illustrated in Fig. 12. The pressure is the major effect on stress at the beginning of time whereas the thermal stress effect increases with time. This relation is reasonable because the pressure fluctuation is damped with time whereas the internal temperature increase is

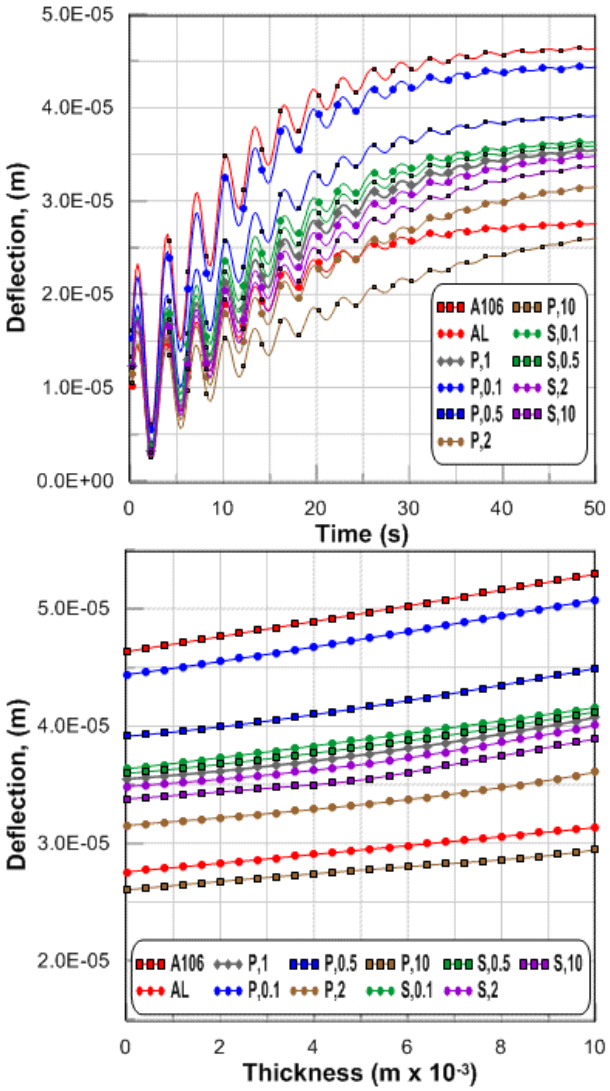

Fig. 13 Deflections according to the material composition under combined load

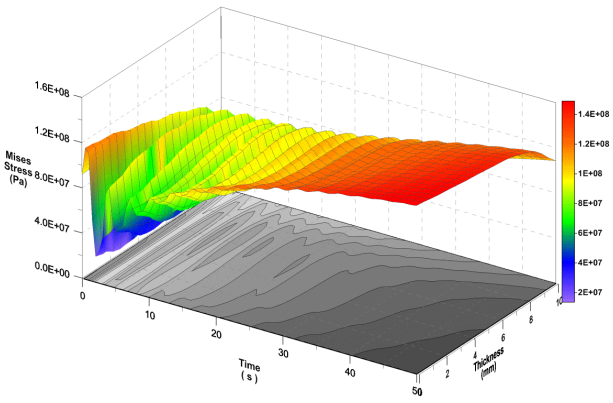

Fig. 14 Stresses at FG pipe according to PFGM and n=10 under combined load

exponentially proportional with the time. The effect of variation of FGM functions and their parameters on the stress and deflection is obvious and the total stresses are clearly improved when the PFGM with n=10 is applied and it has the lowest deflection as shown in Fig. 13.

Applying PFGM with n=10 makes better distribution of Von-Mises stresses through thickness and time as shown in Fig. 14 and it doesn't exceed 150 MPa as shown in Fig. 12.

5. Conclusions

In this study different configuration of FG pipes in addition to the carbon steel and alumina pipes are analyzed to obtain the variation in the transient response when they are subjected to nonlinear and unsteady internal pressure and temperature. FEM is applied. FGM obviously improves the material response to transient loads and enhanced the stress distribution through the pipe wall. The comprehensive study of FGM sigmoidal and power functions and their parameters reveals that when the power index is less than one the stresses increase specially for PFGM more than SFGM. Contrary to that when the power index is more than one where the stresses decrease, the PFGM is better and its stresses are lower than SFGM. The deflection mainly depends on the power index value of FGM and exists between the deflection of Alumina which is very stiff and carbon steel which is more ductile. PFGM with n=10 reduces the stresses effectively, furthermore its fact as a rich ceramic material at the inner side which attain the aim to get a corrosion-erosion resistant material with better characteristics than traditional applied material. Thermal load is the load component which produces the highest stresses at the axial direction, whereas the internal pressure is the load component which produces the highest stresses at the hoop direction. This study proposes a new extension to the FGM analysis by applying the coupled temperature and displacement FEM solution in a FG pipe structure. Numerical results are given to assist and improve the design of natural gas pipeline.

References

Abdelhak, Z., Hadji, L., Daouadji, T.H. and Adda, B. (2016), "Thermal buckling response of functionally graded sandwich plates with clamped boundary conditions", *Smart Struct. Syst.*, **18**(2), 267-291.

Aboudi, J., Pindera, M.J. and Arnold, S.M. (1999), "Higher-order theory for functionally graded materials", *Compos. Part B: Eng.*, **30**(8), 777-832.

Akbarov, S.D., Guliyev, H.H. and Yahnioglu, N. (2017), "Three-dimensional analysis of the natural vibration of the three-layered hollow sphere with middle layer made of FGM", *Struct. Eng. Mech.*, **61**(5), 563-576.

Aldousari, S.M. (2017), "Bending analysis of different material distributions of functionally graded beam", *Appl. Phys. A*, **123**(4), 296.

Alshorbagy, A.E., Eltaher, M.A. and Mahmoud, F.F. (2011), "Free vibration characteristics of a functionally graded beam by finite element method", *Appl. Math. Model.*, **35**(1), 412-425.

Chareonsuk, J. and Vessakosol, P. (2011), "Numerical solutions for functionally graded solids under thermal and mechanical loads using a high-order control volume finite element method", *Appl. Therm. Eng.*, **31**(2), 213-227.

Chi, S.H. and Chung, Y.L. (2002), "Cracking in sigmoid functionally graded coating", *J. Mech.*, **18**, 41-53.

Chikh, A., Bakora, A., Heireche, H., Houari, M.S.A., Tounsi, A. and Bedia, E.A. (2016), "Thermo-mechanical postbuckling of symmetric S-FGM plates resting on Pasternak elastic foundations using hyperbolic shear deformation theory", *Struct. Eng. Mech.*, **57**(4), 617-639.

Daneshjou, K., Bakhtiari, M. and Tarkashvand, A. (2017), "Wave propagation and transient response of a fluid-filled FGM cylinder with rigid core using the inverse laplace transform", *Eur. J. Mech.-A/Sol.*, **61**, 420-432.

Documentation, A.B.A.Q.U.S. (2012), *Simulia*, Providence, RI.

Fazzolari, F.A. (2016), "Reissner's mixed variational theorem and variable kinematics in the modelling of laminated composite and FGM doubly-curved shells", *Compos. Part B: Eng.*, **89**, 408-423.

Fu, Y., Hu, S. and Mao, Y. (2014), "Nonlinear transient response of functionally graded shallow spherical shells subjected to mechanical load and unsteady temperature field", *Acta Mech. Sol. Sin.*, **27**(5), 496-508.

Ghannad, M. and Yaghoobi, M.P. (2017), "2D thermo elastic behavior of a FG cylinder under thermomechanical loads using a first order temperature theory", *J. Press. Vess. Pip.*, **149**, 75-92.

Hamed, M.A., Eltaher, M.A., Sadoun, A.M. and Almitani, K.H. (2016), "Free vibration of symmetric and sigmoid functionally graded nanobeams", *Appl. Phys. A*, **122**(9), 829.

Jafari Fesharaki, J., Madani, S.G. and Golabi, S.I. (2016), "Numerical and analytical investigation of a cylinder made of functional graded materials under thermo-mechanical fields", *J. Mod. Proc. Manuf. Prod.*, **5**(3), 59-68.

Kar, V.R. and Panda, S.K. (2015), "Free vibration responses of temperature dependent functionally graded curved panels under thermal environment", *Lat. Am. J. Sol. Struct.*, **12**(11), 2006-2024.

Khazaeinejad, P. and Usmani, A.S. (2016), "Temperature-dependent nonlinear analysis of shallow shells: A theoretical approach", *Compos. Struct.*, **141**, 1-13.

Liang, X., Wang, Z., Wang, L., Izzuddin, B.A. and Liu, G. (2015), "A semi-analytical method to evaluate the dynamic response of functionally graded plates subjected to underwater shock", *J. Sound Vibr.*, **336**, 257-274.

Liew, K.M., Zhao, X. and Ferreira, A.J. (2011), "A review of meshless methods for laminated and functionally graded plates and shells", *Compos. Struct.*, **93**(8), 2031-2041.

Moosaie, A. (2016), "A nonlinear analysis of thermal stresses in an incompressible functionally graded hollow cylinder with temperature-dependent material properties", *Eur. J. Mech.-A/Sol.*, **55**, 212-220.

Najibi, A. and Talebitooti, R. (2017), "Nonlinear transient thermo-elastic analysis of a 2D-FGM thick hollow finite length cylinder", *Compos. Part B: Eng.*, **111**, 211-227.

Ranjbar, J. and Alibeigloo, A. (2016), "Response of functionally graded spherical shell to thermo-mechanical shock", *Aerosp. Sci. Technol.*, **51**, 61-69.

Sator, L., Sladek, V. and Sladek, J. (2017), "Multi-gradation coupling effects in FGM plates", *Compos. Struct.*, **171**, 515-527.

She, G.L., Yuan, F.G. and Ren, Y.R. (2017), "Research on nonlinear bending behaviors of FGM infinite cylindrical shallow shells resting on elastic foundations in thermal environments", *Compos. Struct.*, **170**, 111-121.

Sheng, G.G. and Wang, X. (2017), "Nonlinear response of fluid-conveying functionally graded cylindrical shells subjected to mechanical and thermal loading conditions", *Compos. Struct.*, **168**, 675-684.

Thai, H.T. and Kim, S.E. (2015), "A review of theories for the modeling and analysis of functionally graded plates and shells", *Compos. Struct.*, **128**, 70-86.

Tounsi, A., Houari, M.S.A. and Bessaim, A. (2016), "A new 3-

unknowns non-polynomial plate theory for buckling and vibration of functionally graded sandwich plate", *Struct*. *Eng*. *Mech*., **60**(4), 547-565.

Viola, E., Rossetti, L., Fantuzzi, N. and Tornabene, F. (2016), "Generalized stress-strain recovery formulation applied to functionally graded spherical shells and panels under static loading", *Compos*. *Struct*., **156**, 145-164.

Wu, C.P. and Lim, X.F. (2016), "Coupled electro-mechanical effects and the dynamic responses of functionally graded piezoelectric film-substrate circular hollow cylinders", *Thin-Wall*. *Struct*., **102**, 1-17.

Wu, C.P. and Liu, Y.C. (2016), "A review of semi-analytical numerical methods for laminated composite and multilayered functionally graded elastic/piezoelectric plates and shells", *Compos*. *Struct*., **147**, 1-15.

CC